J Appl Electrochem (2009) 39:647–652
DOI 10.1007/s10800-008-9704-2

ORIGINAL PAPER

A modified composite film electrode of polyoxometalate/carbon nanotubes and its electrocatalytic reduction

Weihua Guo · Lin Xu · Bingbing Xu · Yanyan Yang · Zhixia Sun · Shuping Liu

Received: 22 July 2008 / Accepted: 22 October 2008 /

Abstract Keggin-type polyoxometalate ($H_4SiMo_{12}O_{40}$) and carbon nanotubes (CNTs) coated by poly(allylamine hydrochloride) (PAH) were alternately deposited on glassy carbon (GC) electrodes by an electrochemical growth method in acidic aqueous solution. The preparation of the film electrode was simple and convenient. Thus-prepared multilayer films and the electrochemical behavior of the composite film modified electrode were characterized by UV–vis spectroscopy and cyclic voltammetry. It was shown that the multilayer films are uniform and stable. The resulting multilayer film modified electrode behaves as an electrochemical sensor because of its low overpotential for the catalytic reduction of $S_2O_8^{2-}$ and NO_2^- in acidic aqueous solution.

Keywords Polyoxometalates · Electrochemical growth · Electrocatalytic · Carbon nanotubes

1 Introduction

Over the last decade, chemically modified electrodes (CMEs) have been intensively used in electroanalysis due to their high sensitivity and excellent selectivity. Since their discovery by Iijima in 1991 [1], carbon nanotubes (CNTs), as a novel type of porous nanostructure material, have been widely studied because of their good physical and chemical properties such as high surface area, exceptional physicochemical stability, high electrical conductivity [2, 3]. The subtle electronic properties of CNTs suggest that they have the ability to promote electron transfer reaction when used as an electrode material, providing a new way for surface modification for designing new electrochemical sensors [4–8]. Furthermore, CNTs modified electrodes have shown interesting electrocatalytic activity for both bioorganic and inorganic compounds such as glutathione, homocysteine, carbohydrates, NADH, hydrogen peroxide [5, 9–12].

On the other hand, polyoxometalates (POMs) have become attractive candidates for CMEs due to their reversible redox activities and excellent electrocatalytic properties [13, 14]. To date, many strategies have been developed to prepare CMEs with a variety of POMs on common solid electrode substrates, such as electrochemical deposition [15, 16], adsorption [17, 18] and entrapment into polymer matrices [19–21]. Among these methods, the multilayer electrochemical self-assembly yields a more uniform and stable product in comparison with the immersion method. Recently, some research has focused on both assembly of POMs on CNTs surfaces and its applications in electrocatalysis [22–25]. However, the preparation of POMs and CNTs modified electrodes by the electrochemical growth method and its application to electrocatalytic reduction have not been reported to date. It could be anticipated that multilayer film modified electrodes consisting of POMs and CNTs should exhibit synergetic effects.

In this work, Keggin-type POM ($H_4SiMo_{12}O_{40}$, abbreviated $SiMo_{12}$) was electrodeposited on a glassy carbon (GC) electrode and was then used as matrix to form multilayer films by the electrochemical growth method with the CNTs coated by Poly(allylamine hydrochloride) (pCNTs). The fabricated electrode was evaluated by UV–vis spectroscopy and cyclic voltammetry. In particular, taking account of the deleterious $S_2O_8^{2-}$ and NO_2^- anions,

---

W. Guo · L. Xu (✉) · B. Xu · Y. Yang · Z. Sun · S. Liu
Key Laboratory of Polyoxometalates Science of Ministry of Education, College of Chemistry, Northeast Normal University, Changchun 130024, People's Republic of China
e-mail: linxu@nenu.edu.cn

their electrocatalytic reduction on the pCNTs-modified electrode was also investigated. The high electrocatalytic activities suggest that such an electrode is a promising tool for the determination of $S_2O_8^{2-}$ and NO_2^- anions.

2 Experimental

2.1 Reagents and apparatus

$H_4SiMo_{12}O_{40} \cdot xH_2O$ (abbreviated as $SiMo_{12}$) was synthesized according to the literature method [26]. Poly(allylamine hydrochloride) (PAH, MW 8,000–11,000), Poly(styrenesulfonate) (PSS MW 70,000), and (3-aminopropyl)-trimethoxysilane were purchased from Aldrich and used as received. All other chemicals were of analytical grade and used without further purification. CNTs with diameters of 15–20 nm were purchased from Tsinghua-Nafine Nano-power Commercialization Engineering Center.

All the electrochemical experiments were performed on a CHI605C Electrochemical Workstation (Shanghai Chenhua Instrument Corporation, China). A three-electrode system was employed with a saturated calomel electrode (SCE) as reference, a platinum foil as the counter electrode and the GC electrode modified with the self-assembled films as the working electrode. All the potentials are quoted against SCE. Doubly distilled water was used in all aqueous solution preparation and washing. The sample solutions were purged with purified nitrogen for at least 15 min to remove oxygen prior to the experiments. Infrared spectra of the sample were recorded with Nicolet Magna 560 FT-IR Spectrometer with KBr plate.

2.2 Preparation of pCNTs

The received CNTs were sonicated with 37% HCl for 2 h to remove the catalysts (support and metal particles). The precipitate was kept overnight and then diluted with deionized water. The obtained mixture was oxidized by refluxing in concentrated HNO_3 and H_2SO_4 (volume ratio of 1:3) for 12 h. The resultant mixture was diluted with pure water to about three times of the original volume and stirred for 24 h, and then separated by centrifuging/washing to pH $\sim$ 7. After being dried in a vacuum at 60 °C, the oxidative CNTs were dispersed in deionized water. The pCNTs were prepared by a reported method [27]. PAH was dissolved in deionized water at a concentration of 0.1 mg mL^{-1}, containing 0.05 M NaCl. Certain amounts of CNTs were dispersed in doubly distilled water with sufficient ultrasonication for about 1 h. When they were dispersed thoroughly, PAH aqueous solution was added. After 3 h, black sediment was observed and separated by centrifugation. The residual PAH polymer was removed by high-speed centrifugation and the complex was rinsed with water at least three times. The collected complex was redispersed in water with mild ultrasonication to produce a stable solution of the complex.

2.3 UV–Visible (UV–vis) Absorption Spectroscopy

UV–vis absorption spectra were recorded using a 756CRT UV–visible spectrophotometer on a quartz slide which was cleaned in a H_2O_2/H_2SO_4 (3:7) bath for 20 min, followed by rinsing with water and drying with a high-purity nitrogen stream. A precursor film was deposited on a cleaned substrate by immersing the substrate alternately in (3-aminopropyl)trimethoxysilane, 10^{-3} M PSS, 10^{-3} M PAH solutions for 2 h, 20 min, and 20 min, respectively, followed by rinsing with deionized water and drying in a gentle nitrogen stream after each immersion. The treated quartz slide was alternately immersed for 20 min in 4 mM $SiMo_{12}$ and the as-prepared pCNTs solution. The resulting films were washed with water, dried under nitrogen and used to record UV–vis spectra to follow the deposition processes.

2.4 Preparation of the modified electrodes

The multilayer film modified electrodes were prepared by the electrochemical growth method developed by Dong et al. [28]. Firstly, the surface of the GC electrode was polished before each experiment with 1.0, 0.3, and 0.05 μm α-Al_2O_3 powder and rinsed with water between each polishing step. Then, it was washed successively with 1:1 nitric acid, acetone, and water in an ultrasonic bath and dried in air. For preparation of the multilayer film modified electrode, the GC electrode was first placed in $SiMo_{12}$ solution (1 mM $SiMo_{12}$ dissolved in 0.1 M H_2SO_4 solution) and at the same time a cyclic potential sweep was conducted in the potential range -0.1 to 0.6 V at a scan rate of 50 mV s^{-1} for 25 cycles. The $SiMo_{12}$ molecules were adsorbed on the GC electrode and the resulting monolayer film had a negative charge. Then, the resulting electrode ($SiMo_{12}$/GC) was placed alternately in pCNTs and $SiMo_{12}$ solutions and in each solution a cyclic potential sweep was conducted simultaneously. Between each modification, the resulting electrode was washed with water, without any need for the drying steps. Finally, the modified electrode was placed in 0.1 M H_2SO_4 solution and scanned for 25 cycles at 50 mV s^{-1} over the range of -0.1 to 0.6 V to obtain a stable response for the surface-immobilized films. The results show that the initial decay observed in all cases for redox response might be due to the release of modifiers that are bound weakly to the surface and can be displaced somewhat easily.

3 Results and discussion

3.1 Characterization of CNTs and pCNTs

To clarify the formation of PAH on the CNTs surface, FT–IR measurements were carried out for the raw CNTs, acid-treated CNTs, and pCNTs composite. The corresponding results are shown in Fig. 1. For the acid-treated CNTs (curve (b) in Fig. 1), two peaks observed at 1,171 and 1,707 cm^{-1} in the range of 500–2500 cm^{-1} are assigned to υ(C–O) and carboxyl groups, respectively. This demonstrates the formation of carboxyl on the surface of the CNTs after being treated with the mixed concentrated acids as compared with curve (a). As shown in Fig. 1c, some characteristic peaks are observed in the IR spectrum of pCNTs, the υ_s(OH), υ_{as}(CH_2), υ_s(CH_2), and υ(C–N) appeared at 3434, 2925, 2852, and 1380 cm^{-1}, respectively. Furthermore, the peak at 1,643 cm^{-1} can be assigned to carboxylate according to the υ_{as}(RCOOR′) at 1,650–1,545 cm^{-1} [29]. The above results verified the formation of pCNT hybrid materials.

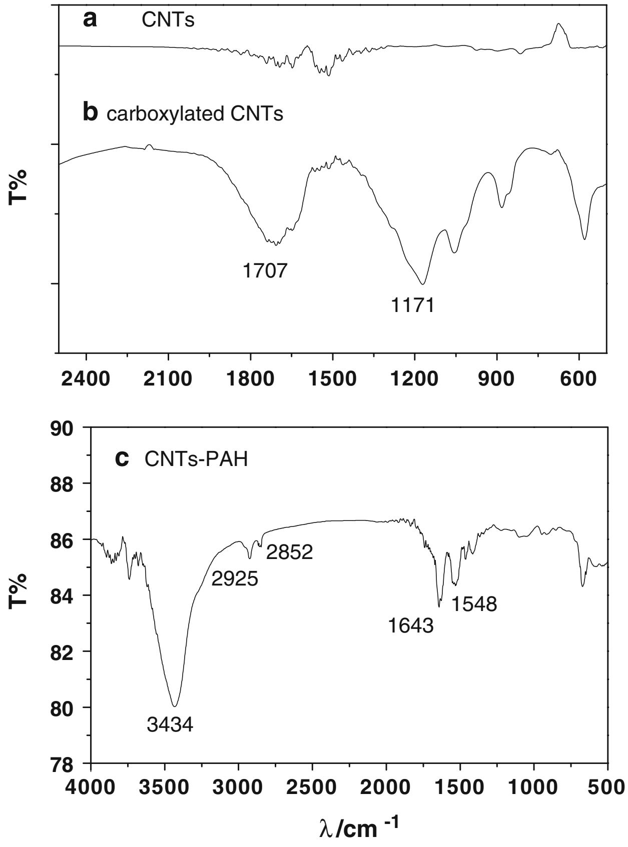

Fig. 1 FT–IR for: **a** raw CNTs, **b** acid-treated CNTs, and **c** pCNTs

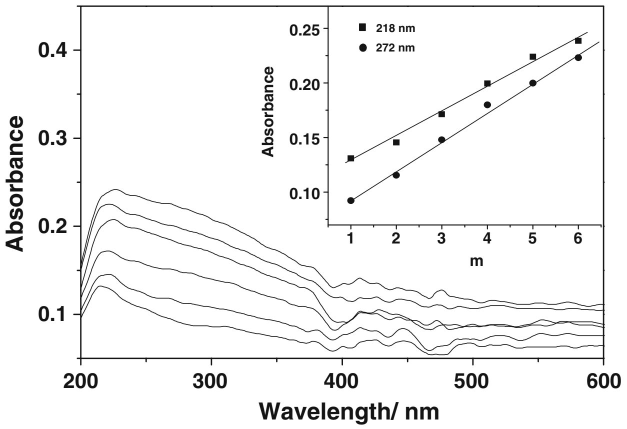

Fig. 2 UV–vis absorption spectra of multilayer films $(\mathrm{pCNTs})_m/(\mathrm{SiMo}_{12})_n$/GC on quartz substrates with $m = 1–6$ (from lower to upper curves). The inset shows the relationship of absorbance at 218 and 272 nm versus the number of layers

3.2 UV–vis absorption spectra for monitoring film growth

Figure 2 shows the UV–vis absorption spectra of the $(\mathrm{pCNTs})_m/(\mathrm{SiMo}_{12})_n$ multilayer films ($m = 1–6$) with pCNTs as the outermost layer. It can be seen that the absorption of the multilayer films occurs at the same wavelength with sequential deposition. The absorbance at 218 nm corresponds to the $O_d \rightarrow$ Mo charge transfer (CT) transition of SiMo_{12} and the broad peak at 272 nm is ascribed to pCNTs [30]. The absorbance values increase linearly with the number of layers as shown in the inset of Fig. 2. This indicates that regular and uniform multilayer films have been constructed and pCNTs are adsorbed on the surface of the substrate.

3.3 Electrochemical behavior of pCNTs/SiMo_{12} composite film electrode

The SiMo_{12} anion of Keggin structure is unstable in neutral and basic aqueous solution and undergoes a series of hydrolysis processes [14]. Therefore, electrochemical studies of the pCNTs/SiMo_{12} composite film electrodes were carried out in acidic aqueous solutions.

Figure 3 illustrates the cyclic voltammograms (CVs) of $(\mathrm{pCNTs})_m/(\mathrm{SiMo}_{12})_n$/GC multilayer films ($\mathrm{SiMo}_{12}$ as outermost layer) with different number of SiMo_{12} layers (from inside to outside corresponding to $n = 1$, 2, 3, 4, and 5, respectively) in 0.1 M H_2SO_4 at scan rate of 50 mV s^{-1}. In the potential range −0.1 to 0.6 V (vs. SCE), there are three couples of redox peaks with formal potentials (E_f) at 0.27 (I), 0.14 (II), and −0.03 V(III), and the peak potential separation $\Delta E_p = E_{pa} - E_{pc}$ are 27, 31, and 26 mV, respectively. Redox peaks I–I′, II–II′, and III–III′ correspond to three consecutive two-electron processes of

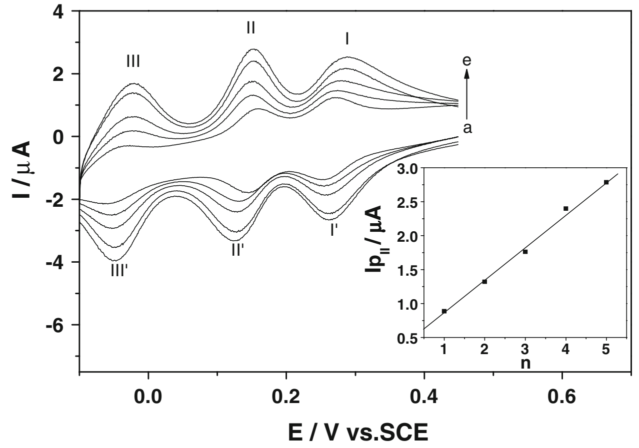

Fig. 3 CVs of $(pCNTs)_m/(SiMo_{12})_n$/GC electrode in 0.1 M H_2SO_4 solution (n = 1–5). Scan rate: 50 mV s^{-1}. Inset: the relationship between peak currents (the second peak) versus number of layers

$SiMo_{12}$. In addition, redox currents increased with the number of layers and the reduction peak potentials shifted to negative slowly. The peak currents increased linearly with the number of layers, as shown in the inset of Fig. 3. This indicates that pCNTs were adsorbed on the surface of the electrode and did not affect the electron transfer between $SiMo_{12}$ and the GC electrode.

Figure 4a shows the CVs of the $(pCNTs)_4/(SiMo_{12})_5$/GC at different scan rates in the potential range −0.1 to 0.6 V in 0.1 M H_2SO_4 solution. The good linearity in the plot of peak currents versus scan rate below 200 mV s^{-1} was observed as expected for a surface confined redox process (Fig. 4b). At higher scan rates, the peak current versus scan rate plots deviate from linearity and the peak currents become proportional to the square root of the scan rate (Fig. 4c) indicating a diffusion-controlled process. Moreover, the E_f does not change with increasing scan rate and the ΔE_p are about 35 mV, suggesting that the electron-transfer kinetics are very fast in the modified electrode surface.

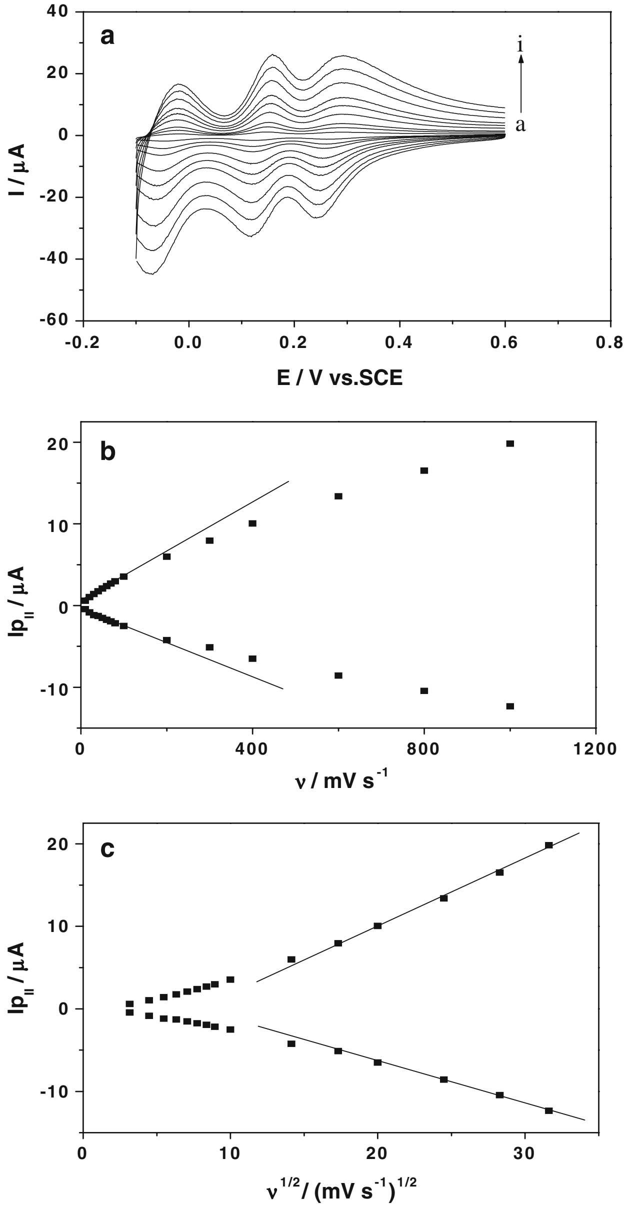

Fig. 4 **a** The CVs of the $(pCNTs)_4/(SiMo_{12})_5$/GC electrode in 0.1 M H_2SO_4 aqueous solution at different scan rates (from a to i: 20, 60, 100, 200, 300, 400, 600, 800, and 1,000 mV s^{-1}); **b** The plot of peak current *vs.* scan rate; **c** The plot of peak current *vs.* square root of scan rate

3.4 pH dependence and stability of pCNTs/$SiMo_{12}$ composite film electrode

pH-dependent electrochemical behavior is commonly found for POMs either dissolved in solutions or immobilized on electrodes [13, 14, 31]. The pH of the supporting electrolyte has a remarkable effect on the electrochemical behavior of the $(pCNTs)_8/(SiMo_{12})_9$/GC electrode. Along with increasing pH, the peak potentials all gradually shift to the more negative potential range and the peak currents decrease, as shown in Fig. 5a. This can be explained by the fact that the reduction of $SiMo_{12}$ immobilized in the composite film was accompanied by the transfer of protons from solution to the surface of the electrode to maintain charge neutrality. When pH increases, slower charge transfer [32] of bulkier cations to the $(pCNTs)_8/(SiMo_{12})_9$/GC electrode should be the reason for the decrease in current, and the more negative reduction potentials can be elucidated by the Nernst equation [33]. Plots of E_f of the three successive redox waves versus pH for the $(pCNTs)_8/(SiMo_{12})_9$/GC electrode exhibit good linearity in the pH range 0.38–4.94 (Fig. 5b). The slopes in this pH range are −54, −74, and −67 mV pH^{-1} for the I–I′, II–II′, and III–III′ couples, respectively, which are close to the theoretical value of −57 mV pH^{-1} for the $2e^-/2H^+$ redox

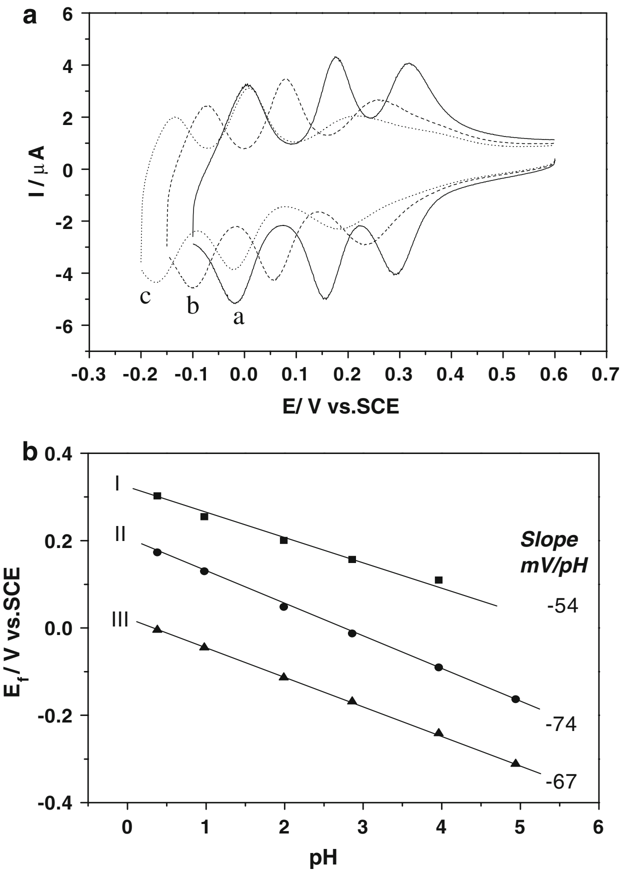

Fig. 5 The CVs of **a** $(pCNTs)_8/(SiMo_{12})_9$/GC electrode in H_2SO_4 aqueous solution at different pH: 0.38 (a); 1.84 (b); 2.88 (c); Scan rate: 50 mV s^{-1}. Plot **b** shows the relationship between formal potentials and pH

process at the experimental temperature. Therefore, the three redox processes of $pCNTs/SiMo_{12}$/GC electrode can be described as follows:

$$H_4SiMo_{12}{}^{VI}O_{40} + 2H^+ + 2e^- \leftrightarrow H_6SiMo_{10}{}^{VI}Mo_2{}^{V}O_{40}$$

$$H_6SiMo_{10}{}^{VI}Mo_2{}^{V}O_{40} + 2H^+ + 2e^- \leftrightarrow H_8SiMo_8{}^{VI}Mo_4{}^{V}O_{40}$$

$$H_8SiMo_8{}^{VI}Mo_4{}^{V}O_{40} + 2H^+ + 2e^- \leftrightarrow H_{10}SiMo_6VIMo_6{}^{V}O_{40}$$

The electrochemical stability of the $pCNTs/SiMo_{12}$ electrode was investigated in 0.1 M H_2SO_4 solution at a scan rate of 50 mV s^{-1}. After 100 cycles, the cathodic peak current (the peak II was used to study) still remains about 93.2% of the first values. These results indicate that the $pCNTs/SiMo_{12}$ electrode has good stability.

3.5 The electrocatalytic activity of the $pCNTs/SiMo_{12}$/GC electrode

Many studies [14] have shown that reduced POMs are capable of delivering electrons to other species, thus serving as powerful electron reservoirs for multi-electron reduction. In our experiments, we chose $S_2O_8{}^{2-}$ and $NO_2{}^-$ as the substrates of analytical interests to test the electrocatalytic properties of the $pCNTs/SiMo_{12}$/GC electrode.

3.5.1 Electrocatalytic reduction of $S_2O_8{}^{2-}$ at $pCNTs/SiMo_{12}$/GC electrode

Since the sulfur compounds play key roles in a number of pathways and biogeochemical processes [34], the determination of sulfur oxoanions is important for industry, medicine and the environment. Here we found that the $(pCNTs)_4/(SiMo_{12})_5$/GC electrode exhibited good electrocatalytic activity toward the reduction of $S_2O_8{}^{2-}$. Figure 6 shows CVs of the $(pCNTs)_4/(SiMo_{12})_5$/GC electrode in 0.1 M H_2SO_4 aqueous solution containing $S_2O_8{}^{2-}$ in various concentrations. The catalytic waves appear on the third (peak III′) reduction waves of $SiMo_{12}$, while the second reduction wave only shows weak electrocatalytic activity toward the reduction of $S_2O_8{}^{2-}$. When the concentration of $S_2O_8{}^{2-}$ increases, the reduction currents of the third waves increase and the corresponding oxidation currents decrease, which indicates that the six-electron reduced species of $SiMo_{12}$ anions present electrocatalytic activity for the reduction of $S_2O_8{}^{2-}$. In this reduction process, the four-electron reduced species is regenerated. The third reductive peak current increases linearly with the concentration of the $S_2O_8{}^{2-}$, as shown in the inset of Fig. 6. The catalytic processes can be shown as follows:

$$H_{10}SiMo_6{}^{V}Mo_6{}^{VI}O_{40}{}^{10-} + S_2O_8{}^{2-}$$
$$\rightarrow H_8SiMo_4{}^{V}Mo_8{}^{VI}O_{40}{}^{8-} + 2SO_4{}^{2-} + 2H^+$$

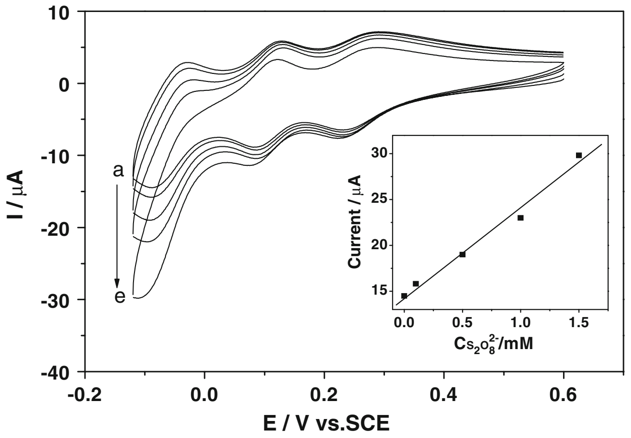

Fig. 6 The CVs of the $(pCNTs)_4/(SiMo_{12})_5$/GC electrode in 0.1 M H_2SO_4 aqueous solution containing (a) 0 mM, (b) 0.1 mM, (c) 0.5 mM, (d) 1 mM, and (e) 1.5 mM $S_2O_8{}^{2-}$. Scan rate: 50 mV s^{-1}. The inset shows the relationship between the third reduction peak current and the concentration of $S_2O_8{}^{2-}$

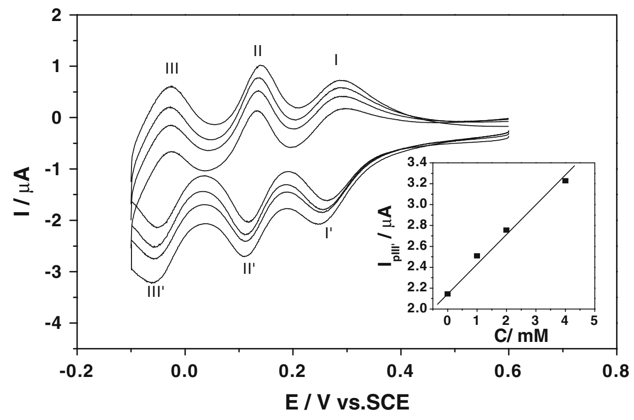

Fig. 7 The CVs of the $(pCNTs)_7/(SiMo_{12})_8$/GC electrode in 0.1 M H_2SO_4 aqueous solution containing (a) 0 mM, (b) 1 mM, (c) 2 mM, and (d) 4 mM NO_2^-. Scan rate: 20 mV s^{-1}. The inset shows the relationship between the third reduction peak current and the concentration of NO_2^-

3.5.2 Electrocatalytic reduction of NO_2^- at pCNTs/SiMo$_{12}$/GC electrode

NO_2^- is a well-known substance which can induce methemoglobinaemia and react with secondary and tertiary amines forming carcinogenic nitrosamines. Therefore, the detection of nitrite in biological denitrification, acid rain, and industrial waste is practically important. The direct electroreduction of nitrite requires a large overpotential at most bare electrode surfaces. POM-modified electrodes have been widely used to decrease the overpotential for the reduction of nitrite. Figure 7 indicates the electrocatalytic reduction of nitrite on a $(pCNTs)_7/(SiMo_{12})_8$/GC electrode in 0.1 M H_2SO_4 aqueous solution. With the addition of nitrite, all the three reduction peak currents increase gradually, whereas the corresponding oxidation peak currents decrease, suggesting that nitrite is reduced by two-, four-, and six-electron reduced species of $SiMo_{12}$ anions. The six-electron reduced species have larger catalytic activity towards nitrite than the two- and four- electron reduced species. The catalytic current taken at the third reductive peak increased linearly with the concentration of the nitrite, as shown in the inset of Fig. 7.

4 Conclusions

Multilayer films composed of pCNTs and silicomolybdate were synthesized on glassy carbon by an electrochemical growth method in acidic aqueous solution. The preparation of the $(pCNTs)_m/(SiMo_{12})_n$/GC electrode is simple and convenient. The resulting multilayer films are uniform and stable. The film modified electrode exhibited good reversibility and could electrocatalyze reduction of $S_2O_8^{2-}$ and NO_2^- in acidic solution. Hence, the modified electrode can be used as an amperometric sensor for the determination of those analytes because of its low overpoential and high catalytic sensitivity.

Acknowledgments The authors are thankful for financial support from the National Natural Science Foundation of China (Grant No. 20671017; 20731002). This work was also supported by the Program for Changjiang Scholars and Innovative Research Team in the University.

References

1. Iijima S (1991) Nature 354:56
2. Ajayan PM (1999) Chem Rev 991:787
3. Sinnott B (2002) J Nanosci Nanotechnol 2:113
4. Yan XX, Pang DW, Lu ZX, Lu JQ, Tong H (2004) J Electroanal Chem 569:47
5. Salimi A, Hallage R (2005) Talanta 66:967
6. Salimi A, Banks CE, Compton RG (2004) Analyst 129:225
7. Girishkumar G, Vinodgopal K, Kamat PV (2004) J Phys Chem B 108:19960
8. Liu J, Tian S, Knoll W (2005) Langmuir 21:5596
9. Gong K, Dong Y, Xiong S, Chen Y, Mao L (2004) Biosens Bioelectron 20:253
10. Deo RP, Wang J (2004) Electrochem Commun 6:284
11. Musameh M, Wang J, Merkoci A, Lin Y (2002) Electrochem Commun 4:743
12. Qian L, Yang X (2006) Talanta 68:721
13. Keita B, Nadjo L (2007) J Mol Catal A: Chem 262:190
14. Sadakane M, Steckhan E (1998) Chem Rev 98:219
15. Keita B, Bouaziz D, Nadjo L, Deronzier A (1990) J Electroanal Chem 279:187
16. Reybier K, Malugani JP, Fantini S, Herlem M, Fahys B (2002) J Electrochem Soc 149:E96
17. Dong S, Wang B (1992) Electrochim Acta 37:11
18. Ca DV, Sun L, Cox JA (2006) Electrochim Acta 51:2188
19. Liu M, Dong S (1995) Electrochim Acta 40:197
20. Bidan G, Genies EM, Lapkowski MJ (1998) J Electroanal Chem 251:297
21. McCormac T, Farrell D, Drennan D, Bidan G (2001) Electroanalysis 13:836
22. Qian L, Yang X (2005) Electrochem Commun 7:547
23. Pan DW, Chen JH, Tao WY, Nie LH, Yao SZ (2006) Langmuir 22:5872
24. Qu JY, Zou XQ, Liu BF, Dong SJ (2007) Anal Chim Acta 599:51
25. Li ZF, Chen JH, Pan DW, Tao WY, Nie LH, Yao SZ (2006) Electrochim Acta 51:4255
26. Rocchiccioli-deltcheff C, Fournier M, Franck R, Thouvenot R (1983) Inorg Chem 22:207
27. Kim B, Sigmund WM (2004) Langmuir 20:8239
28. Cheng L, Niu L, Gong J, Dong SJ (1999) Chem Mater 11:1465
29. Wu JG (1994) Technology and applications of fourier transform infrared spectroscopy, Scientific and Technical Documents Publishing House
30. Zhang MN, Su L, Mao LQ (2006) Carbon 44:276
31. Dong S, Cheng L, Zhang X (1998) Electrochim Acta 43:563
32. Brett CMA, Brett AMO (1993) Electrochemistry principles, methods, and applications. Oxford University Press, Oxford, p 25
33. Wang J (1994) Analytical electrochemistry, VCH, New York
34. Miller PL, Vasudevan D, Gschwend PM, Roberts AL (1998) Environ Sci Technol 32:1269